# Contact Line Dynamics in Drop Coalescence and

# Spreading

R. Narhe, D. Beysens\* and V. S. Nikolayev

Equipe du Supercritique pour l'Environnement, les Matériaux et l'Espace, Service des Basses

Températures, CEA-Grenoble, Grenoble (France)

Mailing address: CEA-ESEME, ICMCB, 87, Av. Dr. A. Schweitzer, 33608 Pessac Cedex (France)

\* To whom correspondence should be addressed. E-mail: <a href="mailto:dbeysens@cea.fr">dbeysens@cea.fr</a>

The dynamics of coalescence of two sessile drops is investigated and compared with the spreading dynamics of a single water drop in partially wetting regime. The composite drop formed due to coalescence relaxes exponentially towards equilibrium with a typical relaxation time that decreases with contact angle. The relaxation time can reach a few tenth of seconds and depends also on the drop size, initial conditions and surface properties (contact angle, roughness). The relaxation dynamics is larger by 5 to 6 order of magnitude than the bulk hydrodynamics predicts, due to the high dissipation in the contact line vicinity. The coalescence is initiated at a contact of the drops growing in a condensation chamber or by depositing a small drop at the top of neighboring drops with a syringe, a method also used for the studies of the spreading. The dynamics is systematically faster by an order of magnitude when comparing the syringe deposition with condensation. We explain this faster dynamics

by the influence of the unavoidable drop oscillations observed with a fast camera filming. Right after the syringe deposition the drop is vigorously excited by deformation modes, favoring the contact line motion. This excitation is also observed in spreading experiments while it is absent during the condensation-induced coalescence.

#### 1. INTRODUCTION

The phenomenon of the coalescence of sessile drops is of critical importance for a number of technological processes. It is also a key phenomenon in the growth of droplets on a surface (Dew, Breath Figures) [1-3]. However, little is known about its dynamics. While the knowledge of the liquid viscosity and surface tension is sufficient to describe the kinetics of coalescence of freely suspended drops, the contact line motion influences strongly the coalescence kinetics of sessile drops. The study of this kinetics is then a tool to study the contact line motion itself.

The contact line motion, i.e. the motion of gas-liquid interface along the solid surface for the case of partial wetting, remains a very active field of study in spite of numerous works that were published on this subject during the last decades. It was found theoretically that the contact line motion was incompatible with the no-slip boundary condition (zero fluid velocity) on the solid surface [4] that causes the diverging dissipation in the near contact line region of the liquid wedge. In reality, the dissipation is high but finite. Consequently, the response of the contact line to external influence is much slower in comparison to that of the bulk fluid. There is still no certainty on the exact microscopic mechanism of the contact line motion. Some results are described satisfactory by one mechanism, some by others. The contact line motion is sensitive to many factors and is an excellent example of the influence of the microscopic phenomena on the macroscopic motion. Among these factors one can list surface defects (geometric and chemical), presence of a liquid film on the solid, the wetting properties, etc. It is extremely difficult to characterize these factors in practice. The wetting properties are characterized by the contact angle. It appears that the experimental error in the contact angle is often so large that its measurements are not certain, as shown by Lander et al.

and Ruijter et al. [5, 6] who obtained quite different values depending on the measurement setup (Wilhelmy balance or sessile drop). Therefore, in the dynamic measurements we prefer to consider well defined contact line position rather than the contact angle.

The capillary spreading of sessile drop due to heterogeneties in solid surface is studied by Shanahan [7]. De Gennes [8] described the spreading of liquid in presence of a precursor film. The precursor film facilitates the spreading and allows the hydrodynamics of spreading to be explained. However, the ellipsometric studies of Voué et al. [9] showed that while the precursor film plays an important role during the spreading in the complete wetting regime, it is absent for the partial wetting regime. These studies were confirmed indirectly by Ruijter et al. [6, 10] and Rieutord et al. [11]. They found that the spreading for the partial wetting regime was much slower that in the complete wetting case meaning that the application of de Gennes precursor film theory led to unphysical values for the parameters of the theory. We conclude from these studies that in a quite common situation of partial wetting, the precursor film is absent and another model of contact line motion should be applied. Several microscopic models by Blake and Haynes [12], Shikhmurzaev [13], Pomeau [14] have been proposed, some accounting for a phase transition in the immediate vicinity of the contact line. Their discussion is out of the scope of this article. We only note that most of them result in the following expression of the contact line velocity  $v_n$  in the direction normal to the contact line as a function of the dynamic contact angle q:

$$v_{n=} \frac{\mathbf{s}}{\mathbf{x}} \left( \cos \mathbf{q}_{eq} - \cos \mathbf{q} \right) . \tag{1}$$

Here  $q_{eq}$  is the equilibrium value of the contact angle, s is the surface tension and x is a model-dependent parameter that we will call the "dissipation coefficient". Another common feature of these theories is that they predict a large x value so that the ratio

$$K = \frac{h}{x},\tag{2}$$

where h is the shear viscosity, is smaller than unity. A small K value means that the dissipation in the contact line region is large with respect to the dissipation in the bulk of the liquid. The study of Andrieu et al. [15] on the coalescence of sessile drops imposed by condensation growth showed extremely small values  $K \approx 10^{-6}$  -  $10^{-7}$ .

It is recognized generally that the static contact line equation should be non-local because the contact line displacement at one point influences its position at other points through the surface tension. In dynamics, the local relations similar to Eq. (1) (where  $v_n$  depends only on the *local* value of  $\mathbf{q}$ ) were considered universal for a long time. Nikolayev and Beysens [16] have developed a non-local dynamic approach and applied it to the analysis of the relaxation of the composite drop formed by the coalescence of two drops. If non-locality is taken into account, Eq. (1) is not valid in the general case where  $\mathbf{q}$  varies along the contact line.

The purpose of this article is two-fold. First, we study the coalescence of water drops on various kinds of substrates under the conditions of partial wetting. Second, we investigate two different ways to initiate the coalescence of the drops, namely condensation growth and syringe deposition on a substrate. One of the common ways to study the contact line dynamics is the observation of the spreading of a deposited drop. During the syringe deposition, an additional energy is necessarily transferred to the drop due to its collision with the substrate. This additional *kinetic* energy accelerates the contact line motion and has to lead to an additional term in (1) because its right hand part is simply a variation of the *potential* energy [6] of the drop. The contribution of this kinetic energy can be checked by comparing two above mentioned ways to initiate coalescence. If the contribution of the kinetic energy is important, the expression of the type (1) is invalid and can not be used for the interpretation of all the exiting data obtained by syringe deposition of low viscosity drops.

#### 2. EXPERIMENTAL

For this study silicon wafers (untreated and treated) and a polyethylene sheet ( $\approx 50~\mu m$  thick) were used as substrates with different average contact angle and hysteresis. The coalescence of two drops is studied either in (i) a condensation chamber, where droplets grow by condensation and coalesce when they touch each other, or (ii) by adding a small drop on top of one of two neighboring drops by a micro-syringe. The method (ii) also enables (iii) spreading of a single drop to be studied.

We will use the water parameters at 20°C: surface tension s = 73 mN/m, shear dynamic viscosity  $h = 10^{-3}$  Pa.s, density r = 1.0 gcm<sup>-3</sup>.

# 2.1. Chamber experiments

In condensation experiments a small piece of cleaned substrate of 1 cm<sup>2</sup> is fixed on a thick electrolytic copper plate by a thin film of water in order to have good thermal contact with the copper plate. The condensation chamber consists of a Peltier-element thermostat enclosed in a Plexiglas box. The surface temperature can be adjusted above, equal or below the dew temperature ( $T_D$ ). The substrate was cooled from the room temperature ( $T_R \approx 23$  °C) to the desired temperature  $T_s$  that was kept in this series of experiments to  $T_s \gg T_R$  - 5 K. The substrate temperature was measured by a K - type thermocouple placed close to the substrate. The chamber was filled with pure  $N_2$  gas saturated with water at room temperature. In order to avoid dust and to saturate the gas,  $N_2$  is bubbled in pure water. The gas flow rate was controlled with a flow meter and kept fixed at 0.60 1/min. The growth and subsequent coalescence of drops (Fig. 1a) were observed with high-resolution black and white CCD camera (COHU, 4910 series, 50 frames/s) attached to an optical microscope (Leica, DMRXE) and recorded on a video recorder. The video images were then analyzed by image analysis software (ImageTool).

#### 2.2. Syringe experiments

We used 0.2 micron filtered distilled water for all experiments. To induce coalescence in the syringe experiments, two water drops of known volume  $V_2$  were deposited very close to each other on a substrate. A small drop of known volume  $V_1$  was deposited on the top of one of the drops, see Fig. 1b. The process of coalescence and relaxation was filmed with a CCD camera equipped with a macrozoom lens and recorded on a video recorder. The initial process of fusion of two drops for both condensation and syringe experiments was observed with a high speed CCD camera (HCC1000 strobe, 1000 frames/s). For the spreading study, a small water drop of known volume  $V_2$  was deposited on the substrate (Fig. 1d). The spreading was also observed after equilibration of a drop on the substrate and subsequent deposition of a small drop (volume  $V_1$ ) on the top of the first (Fig. 1c). The syringe experiments were all performed at open room atmosphere (room temperature and humidity).

## 2.3. Surface properties

The following substrates were used: (i) 50 µm thick polyethylene sheet, (ii) silicon wafers with different surface treatment. The surface properties, which determine the contact angle, are changed on silicon surface using following silanization procedure [17]. The silicon substrates, 1cm x 1cm, are cut from fresh silicon wafer. The wafer is cleaned in (i) acetone for 5 minutes, (ii) ethanol for 5 minutes, and (iii) fresh solution of H<sub>2</sub>O<sub>2</sub> and H<sub>2</sub>SO<sub>4</sub> (1:4) for 30 minutes. Steps (i) and (ii) are performed in ultrasonic bath.

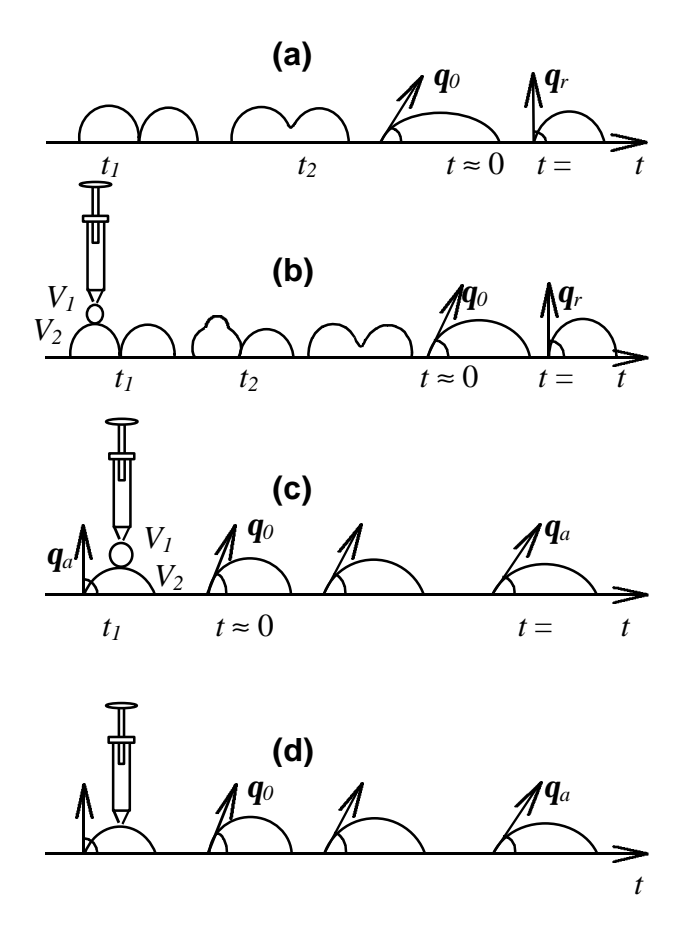


Fig.1. Sketch of (a) coalescence process in condensation experiment, (b) coalescence process in syringe deposition experiment; (c, d) spreading of drop in syringe deposition experiment.

At the end of each step, the wafer is dried by blowing pure dry nitrogen. A small drop of  $50\,\mu l$  of decyltrichlorosilane is put in a cavity of 1.5cm radius and 0.5cm height made (preliminarily) in a Teflon block. The cleaned silicon wafer is placed at distance of 0.5 cm from the top of the block on a height adjustable stand. Since decyltrichlorosilane is volatile, the vapor diffuses and reacts with the wafer's surface. The whole assembly is covered with small glass beaker to prevent the silane vapor from being disturbed. The silanization process time is of 1 min. After silanization the substrate is rinsed with distilled water and dried by blowing dry nitrogen. One can vary the contact angle by changing the stand height (i.e. the

distance between the wafer and the decyltrichlorosilane) while keeping the silanization time constant.

The contact angle of water on a substrate is measured by a sessile drop method. A small drop of 1  $\mu$ l is deposited on the substrate by means of a microliter syringe and visualized using CCD camera with a macro lens. The *static* receding contact angle ( $\mathbf{q}_r$ ) and advancing contact angle ( $\mathbf{q}_a$ ) are measured by adding/removing small amount of water to/from drop with a microsyringe. The value of  $\mathbf{q}_a$  and  $\mathbf{q}_r$  for silicon and polyethylene substrates that we used are given in Table I. We introduce the "equilibrium" value of the contact angle  $\mathbf{q}_{eq} = (\mathbf{q}_a + \mathbf{q}_r)/2$  to characterize a substrate by a single quantity.

Table I. The contact angles and relaxation rates of composite water drop on silicon with various treatment, glass and polyethylene substrates. The  $U^*$  value for Silicon-III was obtained by fitting the data [11] to an exponential relaxation (see Fig. 10).

	$q_r(^\circ)$	$oldsymbol{q}_a(^\circ)$	<b>q</b> <sub>eq</sub> (°)	coales	spreading	
Substrate				Condensation	Syringe	Syringe
				<i>U</i> *(m/s)	<i>U</i> * (m/s)	<i>U</i> * (m/s)
Glass+silane	46	60	53	$(6.5\pm0.4)\cdot10^{-6}$		
from ref. [15]	23	37	30	$(1.2\pm0.1)\cdot10^{-5}$		
Silicon-I	22±2	25±2	23.5	$(2.5\pm0.12)\cdot10^{-5}$	$(1.89\pm0.12)\cdot10^{-3}$	$(1.19\pm0.04)\cdot10^{-2}$
Silicon-I	55±2	79±2	67	$(1.47\pm0.19)\cdot10^{-4}$	$(3.42\pm0.65)\cdot10^{-3}$	$(9.3\pm1.6)\cdot10^{-3}$
+ silane						
Silicon-II	47±2	57±2	52	$(9.74\pm0.12)\cdot10^{-4}$	$(9.54\pm0.7)\cdot10^{-3}$	$(9.3\pm1.6)\cdot10^{-3}$
Silicon-III	10	12	11			$3.65 \cdot 10^{-3}$
from ref. [11]						
Polyethylene	80±2	90±2	85	$(7.24\pm0.7)\cdot10^{-4}$	$(6.15\pm0.6)\cdot10^{-3}$	$(4.1\pm0.9)\cdot10^{-3}$

## 3. RESULTS AND DISCUSSION

#### 3.1. Coalescence in condensation chamber

As sketched in Fig. 1a, the coalescence process is characterized by three time stages.

1. **Formation of liquid bridge** between two drops of radii  $R_1$  and  $R_2$  and subsequent formation of a convex composite drop (between the time moments  $t_1$  and t=0 in Fig. 1a) takes less than 2 ms as shown by Fig. 2a fast camera microscopic picture (silicon II substrate, see Table I for its properties). The drop shape can be characterized by the large axis  $2R_y$  measured in the direction of maximum elongation and the small axis  $2R_x$  measured in the perpendicular direction, where  $R_y$  and  $R_x$  are large and small drop radii, respectively, see Fig. 3. The contact line dynamics is characterized by quick increase of  $R_x$  due to its advancing motion in the "bottleneck" region of the composite drop due to the strong negative drop surface curvature in this region.  $R_y$  remains practically unchanged, i.e. no contact line receding occur. We note that the composite drop relaxes towards equilibrium without visible oscillations.

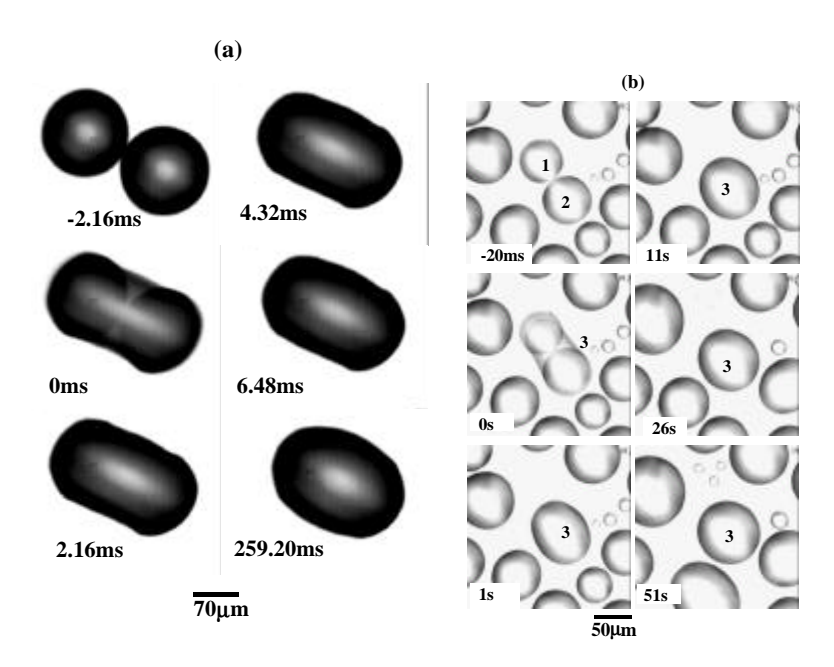


Fig. 2. (a) Fast camera picture of coalescence process on silicon II substrate. The bar corresponds to 70μm. (b) Photo of the coalescence process on silicon-I in a condensation chamber. The bar corresponds to 50μm.

- 2. **Decrease of large radius**  $R_y$  with time and increase of small radius  $R_x$  such that the drop approaches the shape of spherical cap (Figs.2b and 3).
- 3. **Slow growth** of the composite drop by condensation.

We confirm and extend the data on the stage 2 obtained by Andrieu  $et\ al.$  [15]. The composite drop finally becomes hemispherical with equilibrium radius R. The dynamics is very slow and the complete—relaxation takes long time. The relaxation velocity is proportional to the restoring force F which is defined by the variation of the drop surface energy, see Nikolayev and Beysens [16].

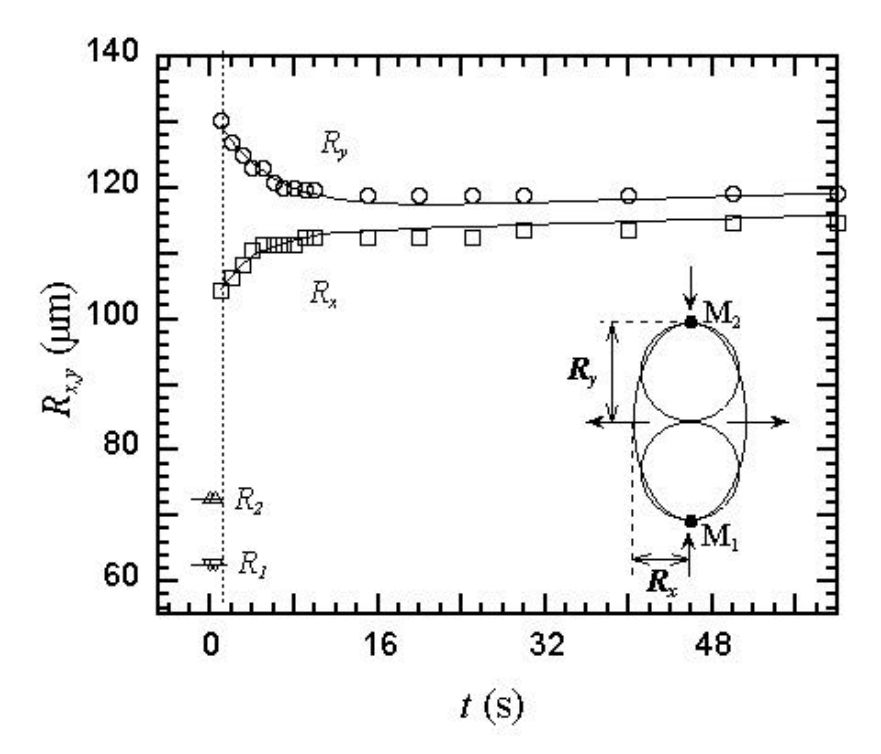


Fig. 3. Evolution of large radius  $R_y$  and small radius  $R_x$  of the composite drop in condensation chamber experiment.  $R_1$  and  $R_2$  are the radii of two drops before coalescence.

On the stage 2 the restoring force f per unit length of the contact line can be approximated by the expression

$$f = \mathbf{S} \left( \cos \mathbf{q} - \cos \mathbf{q}_{r} \right) \tag{3}$$

where q=q(t) is the time dependent dynamic receding contact angle at the points  $M_1$  and  $M_2$  that lie on the long axis (see Fig.3). A rough evaluation of the initial value of this force

$$f_I = \mathbf{S}(\cos \mathbf{q}_0 - \cos \mathbf{q}_r) \tag{4}$$

can be obtained by estimating the initial contact angle  $q_0 = q$  (t=0) at the beginning of the stage 2. To estimate this  $q_0$  angle we assume that during the stage 1,  $R_y$  does not change so that the contact line stays pinned at the points  $M_1$  and  $M_2$ . For the estimation purposes it can be assumed that the composite drop at t=0 takes the spheroid shape which has been described analytically by Nikolayev and Beysens [16]. As it can be seen on Fig. 2b, the image for t = 0 s shows that the small axis is equal to the radius of each of the coalescing drops. One thus postulates  $R_y = 2R_x$ , and one obtains a relationship between the composite drop volume  $V_c$ ,  $R_y$  and  $\cos q_0$  (see Appendix). The volume  $V_c$  can be found by adding the volumes of two identical spherical cap shaped drops (1) and (2) of volume  $V_1 = V_2$ ,  $V_c = 2V_1$ . These drops are assumed to be at equilibrium (i.e. that the contact angle is  $q_a$  after the stage 3 where the contact line advances very slowly due to condensation) just before coalescence begins. Their base radius  $R_1$  can then be obtained from the expression [10]

$$R_1^3 = \frac{3V_1}{\boldsymbol{p}} \frac{(1 + \cos \boldsymbol{q}_a) \sin \boldsymbol{q}_a}{(1 - \cos \boldsymbol{q}_a)(2 + \cos \boldsymbol{q}_a)}.$$
 (5)

Since the points  $M_1$  and  $M_2$  are assumed to be immobile during the first stage,  $R_y = 2R_I$ . For estimation of  $\mathbf{q}_0$ , we use Eq. (A5), as given in the appendix. These equations allow  $\mathbf{q}_0$  and f to be calculated provided  $\mathbf{q}_a$  is given. Its values are reported in Table II. Note that  $\mathbf{q}_0$  is independent of  $V_I$ .

The roughness influence can be estimated by comparing the force calculated in Eq. (4) with

$$f_2 = \mathbf{s} \left( \cos \mathbf{q}_0 - \cos \mathbf{q}_{eq} \right), \tag{6}$$

where the surface roughness influence is neglected. In Fig. 4 we have plotted the forces  $f_{1,2}$  given by Eqs. (4) and (6) with respect to  $\mathbf{q}_{eq}$ . As expected, Eq.(6) gives the larger value for the force.

Table II. The calculated initial contact angle  $q_0$  and the capillary force f per unit length of the contact line in case of coalescence and spreading.

substrate	$oldsymbol{q}_{eq}(^{\circ})$	condensation or deposition coalescence				spreading				
		<b>q</b> <sub>0</sub> (°) calc.	$q_r(^\circ)$	f, mN/m		<b>q</b> <sub>0</sub> (°) calc.	<b>q</b> <sub>0</sub> (°) calc.	<b>q</b> <sub>a</sub> (°)	f, mN/m, Eq. (16)	
				$f_I$ , from	$f_2$ ,	$V_1/V_2$	V <sub>1</sub> /V <sub>2</sub>		$ \begin{array}{c c} V_1/V_2 \\ =1/4 \end{array} $	$V_1/V_2$ =1
				Eq. (4)	from Eq. (6)	= 1/4	= 1			
Glass + silane	53	34.53	46	9.43	23.64					
from ref. [15]	30	19.51	23	1.61	10.51					
Silicon-I	23.5	12.81	22	3.50	5.02	30.7	46.05	25	3.4	15.5
Silicon-I + silane	67	50.42	55	4.64	32.58	88.0	104.7	79	11.3	32.5
Silicon-II	52	32.35	47	11.88	21.91	66.3	85.68	57	10.4	34.3
Silicon-III	11									
from ref. [11]										
Polyethylene	85	61.59	80	22.06	34.73	98.1	113.1	90	10.3	28.6

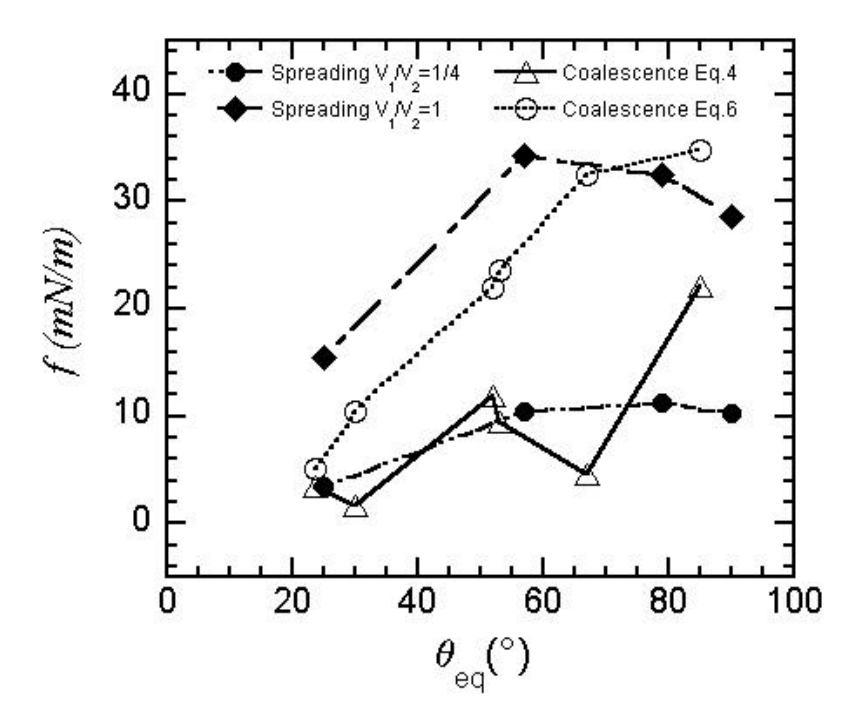


Fig.4. Contact angle dependence of the restoring capillary force f in mN/m as calculated from the experimental data, see Table II.

In Figs. 5 and 6 the relaxation time  $t_c$  versus equilibrium radius R is plotted for silicon I and polyethylene substrates (see Table I for their properties). The relaxation time  $t_c$  is obtained by fitting the relaxation data by an equation of the form

$$R_{x,y}(t) = R_0 \exp\left[\frac{-(t-t_0)}{t_c}\right] + R + A(t-t_0).$$
 (7)

The first term corresponds to the relaxation of the composite drop, which is dominating in regime 2, the second and third term is an expansion that approximately describes the slow growth due to condensation in regime 3. The time where coalescence begins is  $t_0$ . Its experimental value is imposed in the fit.  $R_0$ , R, A,  $t_c$  are the fitting parameters. From Figs. 5 and 6 one can deduce that the relaxation time  $t_c$  follows a linear variation with the final equilibrium radius R of the drop

$$t_c = \left(\frac{1}{U^*}\right) R , \qquad (8)$$

where the parameter  $\boldsymbol{U}^*$  characterizes the contact line relaxation rate.

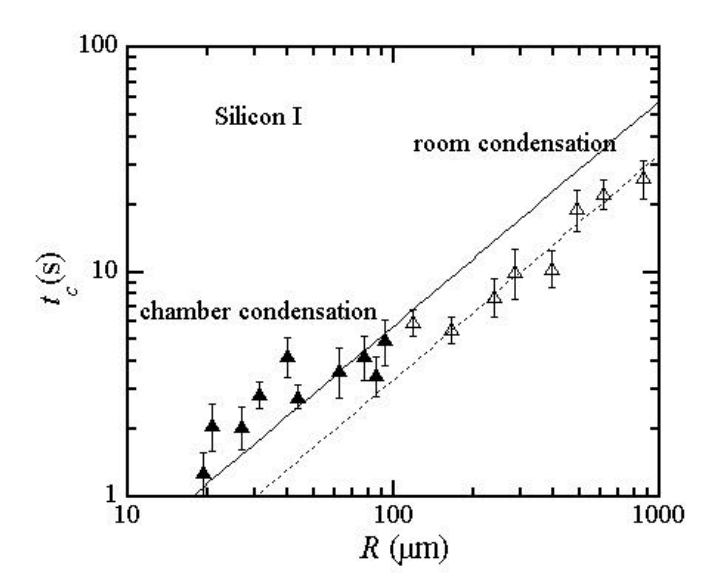


Fig.5. Relaxation time on silicon-I by condensation in chamber and in open room atmosphere at  $T_R$ =23°C,  $T_D$ =18°C,  $T_s$ = $T_D$ -5°C with respect to the equilibrium drop radius R (log-log plot). Lines: best fit to Eq. (8).

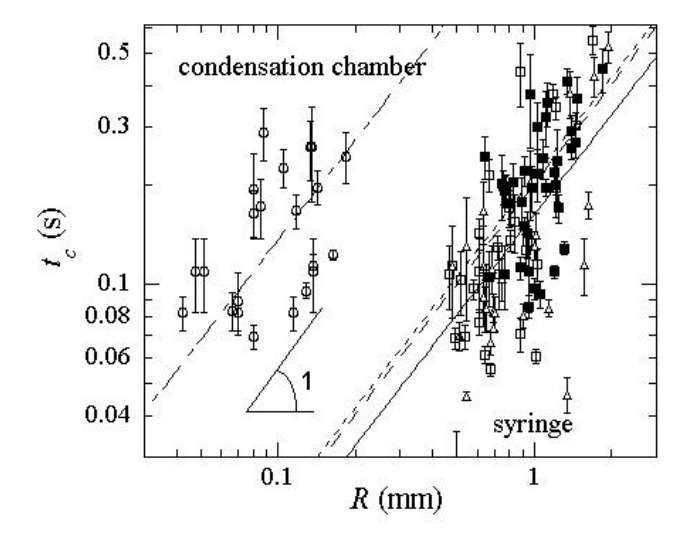


Fig.6. The relaxation time  $t_c$  variations with equilibrium drop radius R for condensation and syringe experiments on polyethylene (log-log plot). The syringe data correspond to different temperature of the substrate around the room dew temperature ( $T_D = 13^{\circ}$ C). Open circles: condensation; open triangles: syringe,  $T_s = T_D + 5^{\circ}$ C; open square: syringe,  $T_s = T_D$ ; full squares: syringe,  $T_s = T_D - 5^{\circ}$ C. Full line: best fit of the data at  $T_s = T_D + 5^{\circ}$ C to Eq. (8). Broken line: best fit of the data at  $T_s = T_D - 5^{\circ}$ C to Eq. (8). Dotted line: best fit of the data at  $T_s = T_D$  to Eq. (8).

 $U^*$  should not be confused with the contact line speed, which obviously varies with time during the relaxation process. The  $U^*$  values obtained for silicon and polyethylene substrate are given in Table I together with data available from literature. It shows that  $U^*$  for silicon surface is one order smaller than for polyethylene. The relaxation dynamics is faster for larger contact angle (for polyethylene) as the restoring force f that moves the contact line is larger (see Table II). This result is in agreement with the predictions of Nikolayev and Beysens [16]. According to them,  $t_c$  should vary with  $\mathbf{q} = \mathbf{q}_{eq}$  as

$$t_c = \frac{1}{K} \frac{\mathbf{h}}{\mathbf{S}} \Phi(\mathbf{q}) R. \tag{9}$$

This defines  $U^*$  as

$$U^* = K \frac{U}{\Phi(q)} \tag{10}$$

with

$$\Phi(\mathbf{q}) = 45 \frac{1 + \cos \mathbf{q}}{(108 + 41\cos \mathbf{q} + 14\cos^2 \mathbf{q} + 17\cos^3 \mathbf{q})(1 - \cos \mathbf{q})}$$
(11)

and

$$U = \mathbf{s/h}.\tag{12}$$

In Fig. 7 the values of  $U^*/U$  are plotted with respect to  $q_{eq}$ . Both condensation and syringe experiments were done many times and each data point was obtained by averaging over 15 to 20 measurements. Although the data exhibit a large scatter, they can be reasonably fitted by the K/F(q) variation (Fig. 7, continuous curve), resulting in the value  $K \approx 2.5 \cdot 10^{-6}$ . The reasons of such a scatter cannot be found in the difference of restoring force due to different  $q_r$ . Indeed, in the framework of a linear approach (see e.g. [15 – 16]) the magnitude of the restoring force cannot influence the relaxation time. The above scatter probably could be explained by the influence of defects. The effect of successive pinning and depinning of the contact line (cf. Fig.9a below) can result either in an increase of the relaxation time (the

contact line stays longer on the defects) or to a decrease (the contact line jumps quickly between the defects). 2-D simulation [16] shows that these two antagonist effects nearly cancel. A non-linear approach (e.g. that of [18]) should be applied to elucidate the collective effect of the defects on the contact line motion.

The size of the drops in the chamber condensation experiments is limited by the minimum microscope magnification (the drops grow out of the field of view). To analyze the growth kinetics on longer time scale we performed the condensation experiments with the same substrate in the open room atmosphere using the observation device used for the syringe deposition. The substrate (of temperature  $T_s$ ) was cooled below dew temperature  $T_D$  to achieve the condensation. The results of these observations are plotted in Fig. 5. They can also be described by (8). However, the  $U^*$  value is slightly different.

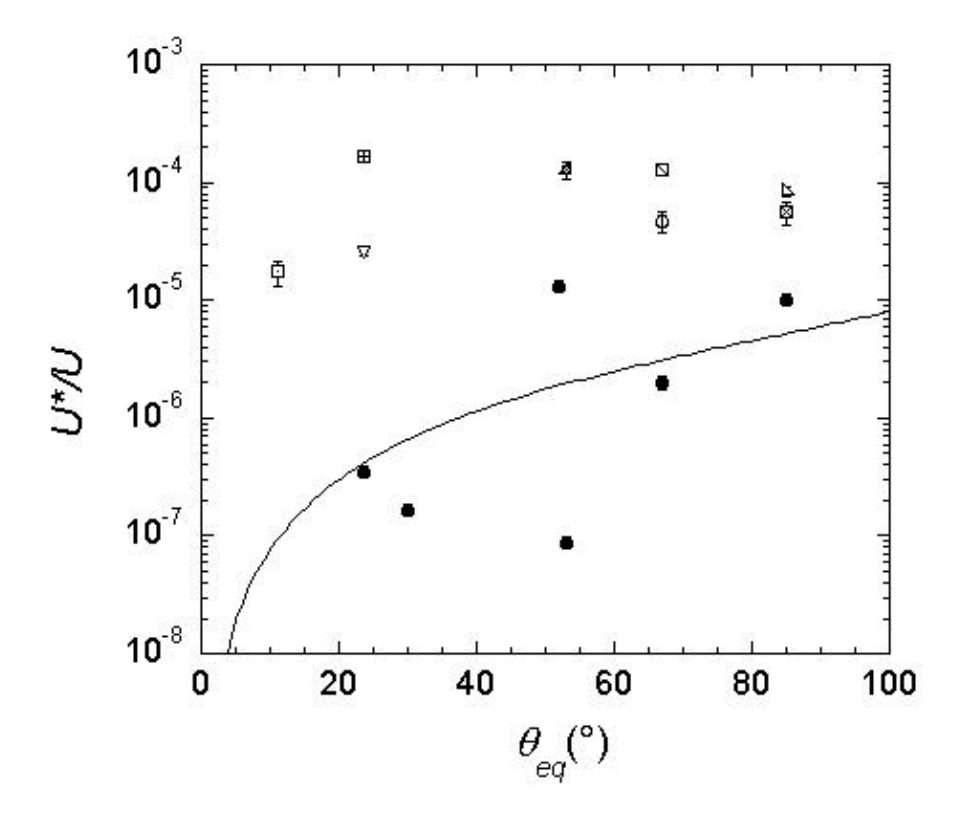


Fig.7. Experimental ratio  $U^*/U$  from Table I with respect to  $\mathbf{q}_{eq}$  for different substrates and coalescence methods (semi-log plot). Full dots: results of chamber condensation. Full curves: best fit of full dots to  $K/\mathbf{F}(\mathbf{q})$ , with  $K = 2.5 \cdot 10^{-6}$ .

Open symbols: syringe experiments. Coalescence:  $\nabla$ , Silicon-I;  $\odot$ , Silicon-I-silane;  $\triangle$ , Silicon-II;  $\triangle$ , Polyethylene. Spreading:  $\boxplus$ , Silicon-I;  $\triangleright$ , Silicon-I-silane;  $\bigcirc$ , Silicon-II;  $\bigcirc$ , Silicon III (Ref. [7]);  $\triangleright$ , Polyethylene. (U = s/h = 73 m/s).

While the chamber condensation results in  $U^* = (3.0 \pm 0.15) \cdot 10^{-5}$  m/s (see solid line in Fig. 5), the coalescence at room atmosphere conditions results in  $U^* = (1.7 \pm 0.16) \cdot 10^{-5}$  m/s (broken line in Fig. 5). This difference can be attributed to the substrate and water contamination impossible to avoid in the open atmosphere.

## 3.2. Coalescence initiated by syringe deposition

After the deposition of third drop at the top of one of the neighboring drops (see Fig. 1b), the relaxation takes place. Since the drop was filmed sidewise in the syringe experiments, the evolution of the smaller drop radius  $R_x$  could not be analyzed. The  $R_y$  data are fitted to the exponential relaxation (7) where the condensation rate A=0. While the restoring force is expected to be similar to that in the condensation experiments (see Table II and Fig.4), the receding is one to two orders of magnitude faster than in the condensation-induced coalescence, see Fig. 6 and Table I. However, the kinetics remains much slower than predicted by bulk hydrodynamics. The value of K is of the order  $10^{-4}$ , cf. Fig. 7.

#### 3.3. Short time coalescence kinetics.

In the syringe deposition coalescence experiments (see Fig. 1b), strong oscillation of the liquid-vapor interface of the composite drop occurs due to the impact with a newly added drop. The drop evolution on Silicon I substrate (see Table I) is filmed with the fast camera (Fig. 8a) and reveals a quick surface motion. Such oscillations are observed commonly when drops are intentionally projected against a substrate [19]. However, to our knowledge such

oscillations were never observed during syringe deposition where the drops are deposited very gently. In Fig. 8b are plotted the time evolution of the heights of the drop profile  $H_L$  and  $H_R$  measured at distances  $0.5R_y$  and  $1.5R_y$  respectively from the left contact point (see Fig.8a). The evolution of  $H_{L,R}$  can be decomposed into exponential relaxation, due to the evolution of  $R_y$  and periodic oscillations whose amplitudes decrease exponentially. The following function

$$H_{L,R} = H_0 + H_1 \exp(-t/t_0) + H_1 \exp(-t/t_1) \cos\left(2p\frac{t}{t} + j\right)$$
(13)

fits correctly the data of Fig.8a. The important parameter of the fits is here the oscillation period t = 7.7 ms (H<sub>L</sub>) and 8.3 ms (H<sub>R</sub>), with uncertainty  $\pm$  0.2 ms. The relaxation times are  $t_0 \approx 16$  ms and  $t_1 \approx 7$  ms. The value of the oscillation period compares well with the period of oscillations of a freely suspended drop of density r:

$$t = \left(\frac{2prR^3}{3s}\right)^{1/2} \tag{14}$$

which gives  $t \approx 10$  ms for R = 1 mm. The latter expression can be obtained easily from the balance of the pressure gradient  $(s/R^2)$  induced by the surface tension and the inertial term  $(r / v/ t) \sim r / t^2$  in the Navier-Stokes equation, with r the density and v the typical interface velocity. A similar value for  $\tau$  was measured by Bahr et al. [19].

Similarly to the long-time  $R_y$  data, the short-time data can also be successfully fitted to the exponential relaxation (7) with A=0. However, the relaxation time  $t_c$  = (2.6 ±0.13) ms turns out to be much smaller: that calculated from the long time relaxation data from Table I, resulting in  $t_c = R/U^* \approx 100$  ms (syringe experiments) or  $t_c \approx 1$  s (condensation chamber).

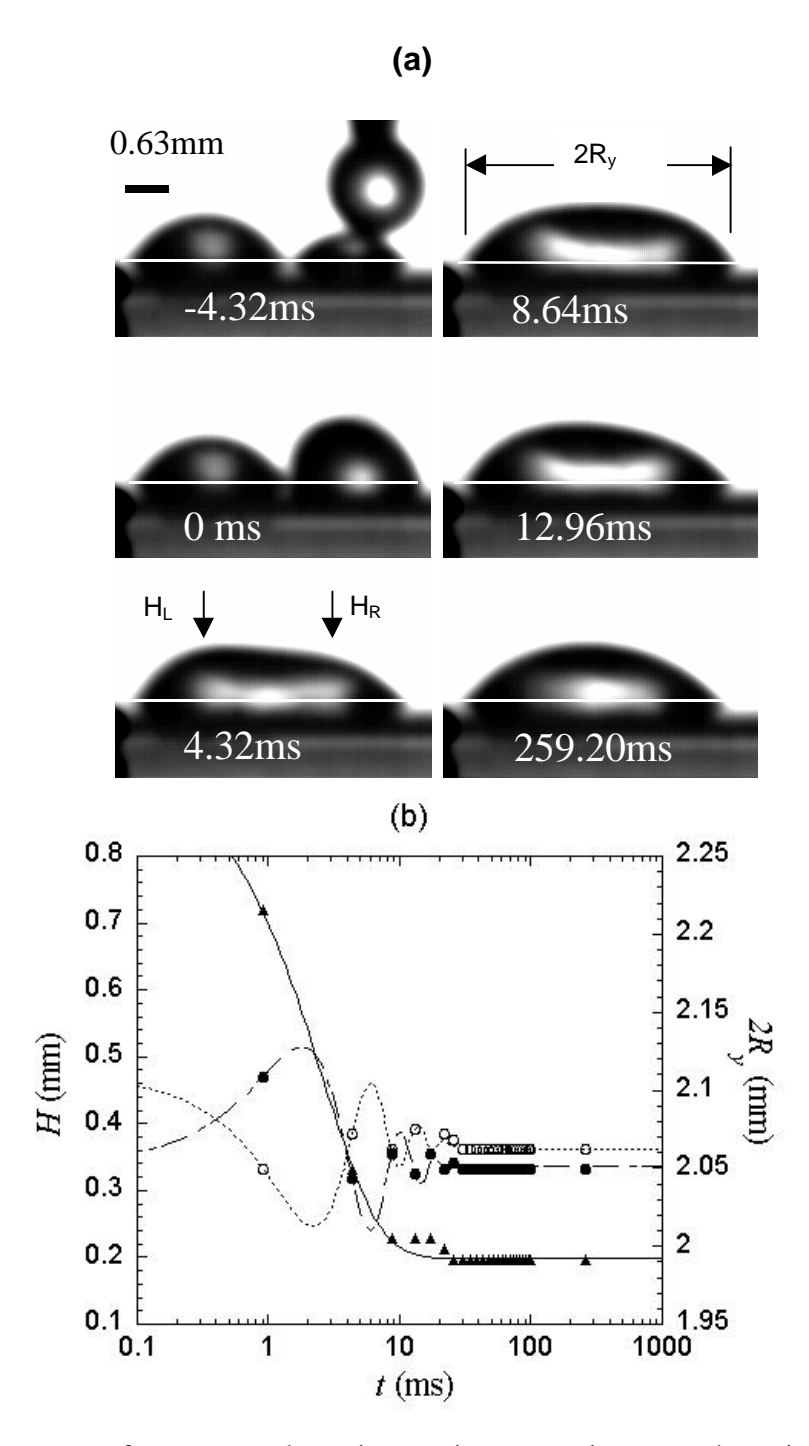


Fig. 8. (a) Coalescence of two water drops in a syringe experiment at short time scale. Photos are taken with a fast camera on silicon I substrate. The volumes of three drops in the t = -4.32ms image are  $0.7\mu$ l,  $0.25\mu$ l and  $0.23\mu$ l. The white horizontal line indicates the substrate surface. The reflection is visible below this line.  $H_L(H_R)$  represents the height of the composite drop on the left (right) side as indicated by the arrows. (b) Evolution of  $H_L$  (open

circles,  $H_R$  (full circles) and  $2R_Y$ .(full triangles) in a semi-log plot. The broken lines are the fits to Eq. (13) and the full line to Eq. (7), with A=0.

This difference can be explained by the influence of the oscillations on the contact line motion. During the oscillations, the contact line is pulled by the drop surface. In Fig.8, one can see a strong correlation between the end of the oscillations and the end of the drop relaxation. It means basically, that in the case of the syringe deposition, the moving force of the contact line motion is related to the kinetic energy of the drop surface motion instead of the potential surface energy. This potential energy is used as a basis to derive the expression (6) for the restoring force and (1) for the contact line velocity [6], which means that both (1) and (6) are not valid description of the spreading by syringe deposition of low viscosity drops. The total duration of this "oscillation stage" of a freely suspended drop would be of the order of the bulk viscous damping time  $R^2r/h \sim 1s$ . In the case of the sessile drop the oscillation damping is faster due to the additional dissipation in the contact line region.

The faster oscillation-induced relaxation on the short time scale should result in a faster relaxation to the spherical cap shape when comparing to the case with no oscillations. In fact, we were not able to detect such oscillations in the condensation experiments and the relaxation time is indeed one to two orders of magnitude larger in the latter case.

#### 3.4. Estimation of the characteristic scale for surface roughness.

From the long time relaxation data, it is possible to study the statistics of the surface roughness. In Fig. 9a, the relaxation of coalescence is shown for drops of about 1.3 mm radius on silicon I + silane substrate (see Table I).

Pinning of the contact line on the defects leads to the "stick-slip" motion clearly seen in Fig.9a. as "slips" or jumps with amplitude **D**R. For small times, where the moving force is

stronger, the line can jump several defects at a time and DR is large. Near the end of the relaxation, DR is small and can be a measure of the average distance between the defects,

$$\boldsymbol{d} = \min\left(\boldsymbol{D}R\right). \tag{15}$$

In Fig. 9b the d values are plotted for various R. There is no visible R dependence. The statistics of these d is shown in Fig.9c, which gives as mean size  $d = 13 \mu m$ .

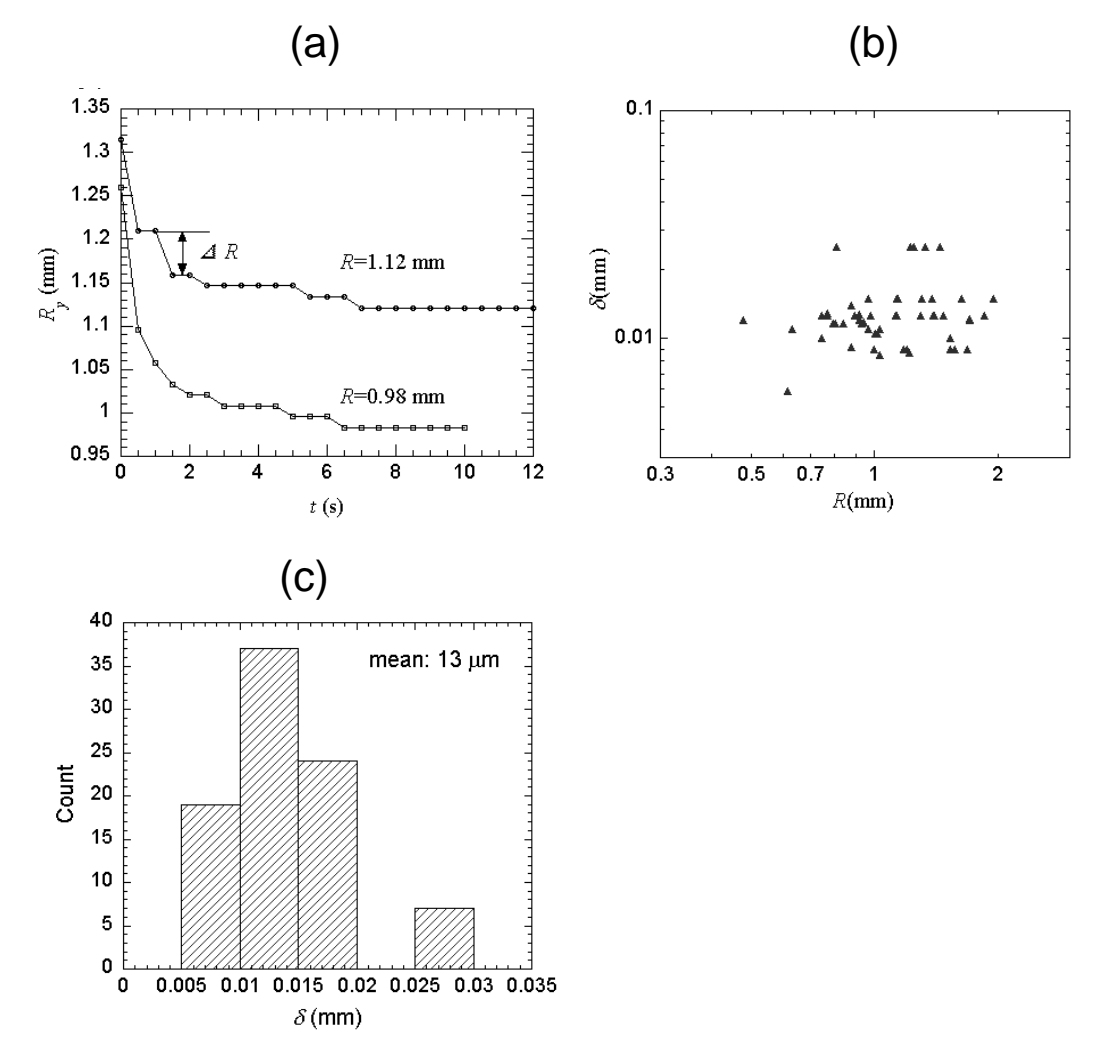


Fig.9. Pinning of the contact line (syringe deposition, silicon I + silane,  $V_1/V_2 = 1/4$ ) during the coalescence. (a) Effects on relaxation. The slips DR are due to pinning on defects. (b) Amplitude (15) of the last slips obtained in multiple experiments on the same substrate as a function of R, in a semi-log plot. (c) Histogram of the amplitude (15) of the last slips from Fig. 9b.

#### 3.5. Influence of the supersaturation

In order to test a possible influence of mass transfer on the contact line motion predicted by Shanahan [20], the syringe experiments were carried out at different temperatures of the substrate  $T_s$  such that  $T_s > T_D$ ,  $T_s = T_D$ ,  $T_s < T_D$ , where  $T_D$  denotes the dew temperature. Changing the substrate temperature modifies the supersaturation at the substrate level and then the intensity of the condensation or evaporation. In our experiment,  $T_s > T_D$  means HR <100%, and drop evaporation occurs, and  $T_s < T_D$  corresponds to supersaturation, and condensation starts on the drop surface and the substrate. The results of these experiments are presented in Fig. 6. We conclude from it that within the accuracy of our experiments, the change in the condensation/evaporation rate does not affect the contact line motion.

Note that when  $T_s < T_D$ , tiny condensing drops are visible on the substrate, some of them coalesce with the composite drop formed during the coalescence of two deposited drops. The volume change of the composite drop due to these multiple coalescences is negligible and the kinetics of the triple line motion is not affected by the presence of these tiny drops.

#### 3.6. Spreading initiated by syringe deposition

The schemes of the spreading experiments are shown in Figs. 1c and 1d. We noticed that for both cases the results are comparable. The fast camera filming of the spreading also shows fast drop surface oscillation analogous to that observed during the coalescence initiated by syringe deposition. Figure 10 reports  $R_y = R_x$  data plotted with respect to t for spreading of a water drop on the silicon I surface in the syringe experiment. The relaxation time is obtained by fitting the data by the exponential function (7) with A=0.

We can compare the spreading relaxation with that observed by Rieutord *et al.* [11] when they are fitted to the same exponential relaxation. Both sets of data clearly fit well an exponential relaxation, with values of  $U^*$  in the same range magnitude (Fig. 10). The Rieutord *et al.* data

show the larger values and the larger data scatter. This is because in Rieutord *et al.* experiments the contact angle was half of the smallest of ours, see Table I. The defect influence is stronger at small contact angles as shows the analysis of the restoring force performed below.

The initial restoring force in the advancing-controlled spreading case can be calculated using the expression

$$f = \mathbf{s} \left( \cos \mathbf{q}_0 - \cos \mathbf{q}_a \right), \tag{16}$$

where the initial contact angle  $\mathbf{q}_0$  is related to  $R_y$  through the expression (5) in which  $\mathbf{q}_a$  is replaced by  $\mathbf{q}_0$ . The volume ratio  $V_1/V_2$  of the added drop  $(V_1)$  at the top of the other  $(V_2)$  was varied from 1/4 to 1 to show the influence of this ratio on the restoring force. When  $V_1/V_2$  is larger, the difference between  $\mathbf{q}_a$  and  $\mathbf{q}_0$  should be larger, which provides a larger f value and thus a quicker relaxation.

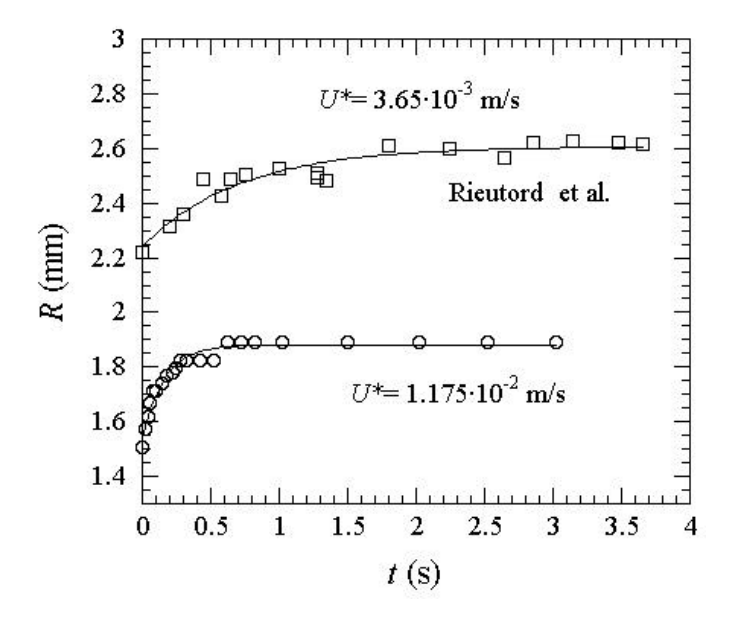


Fig. 10. R with respect to t for spreading of a water drop on silicon I surface in the syringe experiment (circles) and the data of Rieutord et al. [11] (squares). The fits to the exponential relaxation and the resulting  $U^*$  values are shown too. For syringe experiment (circle),  $V_1/V_2 = 1/4$ .

To estimate the initial contact angle  $q_0$  for the spreading of a single drop of volume  $V_2$  by adding new drop of volume  $V_1$ , we assumed that at t = 0 (Fig.1.c), the contact line of drop of volume  $V_2$  stays pinned at the three phase contact line, and its volume increases due to the additional volume of the newly added drop, so that the total volume of the new drop is  $V_1 + V_2$ . By using spherical cap approximation, by knowing volume  $V_2$ ,  $V_1$  and the base radius R of initial drop of volume  $V_2$ , we can calculate the initial contact angle  $q_0$ . The f data are shown in Table II and in Fig.4 for the sake of comparison.

One can notice that the larger  $V_1/V_2$  results in the stronger restoring force value. Fig.4 shows that the restoring force is small for the small contact angles. Therefore, the defects with the same pinning strength influence the relaxation at small contact angle stronger than for the large contact angles. As shown in [16], the defect influence leads to the paradoxous decrease of the total relaxation duration, which manifests itself in a slight  $U^*$  increase.

The relaxation rate  $U^*$  is similar to that for the receding syringe experiments with coalescence (Table I and Fig.7). The relaxation rate in both experiments is 10-100 times larger than for the condensation experiments. We attribute this difference to the additional energy brought to the system due to the impact of the drop during the syringe deposition process. This impact induces the oscillations of the composite drop surface, which create the additional (to f) pulling force acting on the contact line.

#### 4. CONCLUSION

These experiments show that the dynamics of low viscous sessile drops during spreading and coalescence can be markedly affected by initial conditions. In particular, the relaxation rate depends also on the initial kinetic energy given to the drop at the beginning of its relaxation. The syringe deposition induces strong oscillations of the drop. At each oscillation, the drop

surface "pulls" the contact line which thus accelerates its motion. In contrast, drop oscillations are not detected for the case of coalescence observed during the condensation and the relaxation turns out to be 10-100 times slower. This means that the contact line motion studies carried out with the traditional drop deposition method are not accurate enough because of uncontrollable oscillations, important especially for low viscosity fluids. The condensation-induced coalescence presents a more reliable way to study the contact line motion because the oscillations do not occur.

On the other hand, within the accuracy of the experiment, there is no visible influence of the condensation/evaporation kinetics on the contact line motion.

It is very difficult to assign a precise value for the ratio K=h/x, which is found to be of the order  $10^{-4}$  for the syringe deposition and  $2.5 \cdot 10^{-6}$  in the condensation coalescence. Such small K values clearly show that the dynamics of low viscous sessile drops (spreading, coalescence) in the regime of partial wetting is limited by the dissipation at the region of the drop close to the contact line. This dissipation leads to relaxation 5 to 6 orders of magnitude slower than expected from bulk dissipation, a value which cannot be compared easily from the current theories, except the Pomeau expectation that K is a thermally activated Arrhenius factor[14]; however, in this theory, spreading is expected much faster than receding as the Arhenius factor is no longer present. We were unable to put in evidence such a difference in our experiments since spreading studies can be performed only with syringe deposition, which are unreliable because of the drop oscillations.

The relaxation rate was seen to increase with the contact angle, leading to an angle variation in reasonable agreement with the theory of sessile drop relaxation by two of us (V. N. and D. B. [16]).

#### **APPENDIX: Estimation of the initial receding contact angle**

Following Nikolayev and Beysens [16], we approximate the composite drop shape by that of the spheroidal cap defined by the equation

$$x^2/a^2 + [y^2 + (z+d)^2]/b^2 = 1, \quad z > 0,$$
 (A1)

in the Cartesian coordinates (x,y,z). The parameters a,b,d can be found from the following equations (see [16] for more details on them). The first of them fixes the drop volume  $V_c$ :

$$V_c = \frac{\mathbf{p}}{3} \frac{a}{b} (2b^3 - 3b^2 d + d^3) \tag{A2}$$

Next two equations rely a,b and d to the parameters  $R_x$  and  $R_y$ :

$$R_y^2 + d^2 = b^2$$

$$R_y b = R_y a$$
(A3)

The initial receding angle is then defined by the expression

$$\cos \mathbf{q}_0 = d/b.$$
 (A4)

By using the assertion  $2R_x = R_y$  (meaning that the small axis is equal to the radius of each of the coalescing drops, which verifies experimentally, see Fig. 2b, the image for t = 0 s) one finds out easily the equation

$$V_c = \frac{\mathbf{p}}{6} R_y^3 \frac{\sqrt{1 - \cos \mathbf{q}_0} (2 + \cos \mathbf{q}_0)}{(1 + \cos \mathbf{q}_0)^{3/2}}$$
(A5)

that should be solved numerically for  $\cos q_0$  while  $R_v$  and  $V_c$  are known.

#### **ACKNOWLEDGEMENT**

We thank F. Rieutord for giving us his experiment data files and provided us with CEA-LETI silicon wafers and are grateful to Y. Pomeau for exciting discussions. We are indebted to F. Palencia for helping us with the video acquisition apparatus.

#### **REFERENCES**

- 1. D. Beysens and C. M. Knobler, *Phys. Rev. Letts.***1986**, 57, 1433.
- 2. D. Beysens, Atmos. Res., 1995, 39, 215.
- 3. B. J. Briscoe and K. P. Galvin, J. Phys. D: Appl. Phys. 1990, 23, 422.
- 4. C. Huh and L.E. Scriven, J. Colloid Interface Sci. 1971, 35, 85.
- 5. L. M. Lander, L. M. Siewierski, W. J. Brittain and E. A. Vogler, *Langmuir* 1993, 9, 2237.
- 6. M.J. de Ruijter, J. De Coninck, T.D. Blake, A. Clarke and Rainkin, *Langmuir* **1997**, *13*, 7293.
- 7. M. E. R. Shanahan, J. Phys. D: Appl. Phys. 1990, 23, 321.
- 8. P.G. De Gennes, Rev. Mod. Phys. 1985, 57, 827.
- 9. M. Voué, M. P. Valignat, G. Oshanin, A.M. Cazabat, and J. de Coninck, *Langmuir* 1998, 14, 5951.
- 10. M.J. de Ruijter, J. De Coninck and G. Oshanin, Langmuir 1999, 15, 2209.
- 11. F. Rieutord, O. Rayssac and H. Moriceau, *Phys. Rev. E* **2000**, *62*, 6861.
- 12. Blake T.D. and Haynes, J. colloid Interface Sci. 1969, 30, 421.
- 13. Y. D. Shikhmurzaev, *Phys. Fluids* **1997**, *9*, 266.
- 14. Y. Pomeau, C. R. Acad. Sci. IIb, 2000, 238, 411.

- 15. C. Andrieu, D. A. Beysens, V.S. Nikolayev and Y. Pomeau, *J. Fluid. Mech.* **2002**, *453*, 427.
- 16. V. S. Nikolayev and D. A. Beysens, *Phys. Rev. E* **2002**, *65*, 46135.
- 17. Zhao H. and D. Beysens, *Langmuir* **1995**, *11*, 627.
- 18. V. S. Nikolayev and D. A. Beysens, *Europhys. Lett.* **2003**, *64*, 763.
- 19. M. von Bahr, F. Tiberg and B. Zhmud, Langmuir 2003, 19, 10109.
- 20. M. E. R. Shanahan, C. R. Acad. Sci. 2, Sér. 2001, IV, 157.

# For Table of Contents Use Only

Contact Line Dynamics in Drop Coalescence and Spreading R. Narhe, D. Beysens and V. Nikolayev

